Pathogenic mycobacteria manipulate host low density lipoprotein metabolism

Matt D. Johansen[1, 2], Elinor Hortle[2], Joshua Kasparian[1, 2], Alejandro Romero[3], Beatriz Novoa[3], Antonio Figueras[3], Warwick J. Britton[2, 4], Kumudika de Silva[1], Auriol C. Purdie[1], Stefan H. Oehlers[2, 4 *]

[1] Sydney School of Veterinary Science, Faculty of Science, The University of Sydney, Camden, NSW, Australia

[2] Tuberculosis Research Program, Centenary Institute, Camperdown, NSW, Australia

[3] Institute of Marine Research (IIM), Spanish National Research Council (CSIC), Vigo, Spain

[4] Sydney Medical School, The University of Sydney, Newtown, NSW, Australia

[*] Corresponding author: s.oehlers@centenary.org.au

Abstract

Foam cells are a hallmark of mycobacterial infection. Despite their importance to mycobacterial infections, the exact molecular mechanisms underpinning the conversion of macrophages to foam cells *in vivo* are currently unknown. Using the zebrafish embryo-*Mycobacterium marinum* model, we have defined a conserved role for infection-induced altered host lipid metabolism in mycobacterial pathogenesis. Depletion of LDLR, a key lipid metabolism node, decreased *M. marinum* burden, and corrected infection-induced altered lipid metabolism resulting in decreased LDL and a reduced rate of macrophage transformation into foam cells. Our results demonstrate a conserved role for host lipid metabolism and LDLR in mycobacterial pathogenesis.

Footnotes

The authors have no conflicts of interest to report.

This work was supported by the Australian National Health and Medical Research Council (APP1099912 and APP1053407 to S.H.O.); Meat and Livestock Australia (P.PSH. 0813 to A.C.P. and K. dS); the Marie Bashir Institute for Infectious Diseases and Biosecurity (grant to S.H.O., A.C.P. and K. dS); and the Kenyon Family Inflammation Award (grant to S.H.O.), Consellería de Economía, Emprego e Industria (GAIN), Xunta de Galicia (grant IN607B 2016/12 to Institute of Marine Research (IIM-CSIC)).

Meetings: this work has been presented at the 19th Australia and New Zealand Zebrafish Meeting in Wollongong, NSW, Australia.

Corresponding author: Dr Stefan Oehlers. Tuberculosis Research Program, Centenary Institute, Locked Bag 6, Newtown, NSW 2042, Australia. Email: s.oehlers@centenary.org.au

Background

Host lipid metabolism is an important target for subversion by pathogenic mycobacteria such as *Mycobacterium tuberculosis* (*Mtb*). Mycobacteria drive the transformation of infected macrophages into foam cells through the imbalance of low density lipoprotein (LDL) influx and efflux mechanisms (Cardona et al. 2009). Given the significant proportion of the mycobacterial genome that is allocated to lipid metabolism, and the utilisation of lipids such as cholesterol for growth *in vitro*, the abundance of neutral lipids contained within the harsh granuloma microenvironment may supply a carbon source for intracellular mycobacterial survival and persistence (Pandey and Sassetti 2008).

Dyslipidaemia and foam cell differentiation are known to contribute to disease pathology and prognosis in human *Mtb* infection (Dong et al. 2017). However, the involvement of foam

cells in the pathogenesis of non-tubercular mycobacterial infections such as *Mycobacterium avium* subspecies *paratuberculosis* (MAP) or *Mycobacterium marinum* has not been explored. Our group has identified infection-induced changes to host lipid metabolism genes in MAP-infected cattle and aberrant host lipid metabolism gene expression and intracellular cholesterol accumulation within MAP-infected macrophages (Johansen et al. submitted-b; Thirunavukkarasu et al. 2014). Here, we have turned to the natural host-pathogen pairing of the zebrafish-*M. marinum* platform to investigate the conservation of altered host lipid metabolism as a conserved motif across mycobacterial infections.

Zebrafish (*Danio rerio*) are a powerful animal model to study early host-pathogen interactions. Zebrafish demonstrate a functional innate immune system from early in embryogenesis with a high degree of homology to mammals (Traver et al. 2003). *M. marinum* is a natural pathogen of fish and amphibian species and genomic analysis has identified *M. marinum* as the closest genetic relative of the *Mtb* complex, sharing 85% of orthologous regions with *Mtb* (Stinear et al. 2008). The zebrafish-*M. marinum* platform has been used extensively to model host-pathogen interactions relevant to *M. tuberculosis* pathogenesis (Ramakrishnan 2012).

The aim of this study was to explore the biological significance of the key lipid metabolism node Low Density Lipoprotein Receptor (LDLR) in non-tubercular mycobacterial infections. Our findings demonstrate LDLR-mediated uptake of lipids plays an important role in the establishment of mycobacterial infection by manipulating host lipid metabolism and aiding the transformation of macrophages into foam cells.

Methods

Zebrafish maintenance and breeding

Adult zebrafish were housed at the Garvan Institute of Medical Research and maintained under standard zebrafish conditions. Animal ethics for zebrafish experiments was covered under Sydney Local Health District protocols 2016/022 and 2016/037.

Morpholino design and microinjection

Splice-blocking morpholino oligonucleotide for *LDLR* (gene variant *ldlra*) was designed from Ensembl transcript sequences (http://www.ensembl.org/index.html) and purchased from Gene Tools. The *LDLR* morpholino (5'-ATCACATTTCATTTCTTACAGCAGT-3') was targeted at the exon 4/intron 4 and 5 splice junction that was expected to cause the excision of exon 4. The control morpholino (5'-CCTCTTACCTCAGTTACAATTTATA-3') is a negative control targeting a human beta-globin intron known to cause little phenotype variations in zebrafish.

Embryos at the 1-4 cell stage were injected with 2 nL of morpholino into the yolk. Embryos were raised at 28°C in E3 media.

Mycobacterial infection

At 30 hours post-fertilisation, zebrafish larvae were anaesthetised with 160 µg/mL tricaine (Sigma-Aldrich) and infected with approximately 200 CFU wasabi-expressing M strain *M. marinum* via caudal vein injection.

Quantification of *M. marinum* burden

Embryos were anaesthetised with tricaine and imaged on a Leica M205 FA Fluorescent Stereo Microscope (Leica Microsystems). Infection burden was measured as the number of pixels in each embryo above background fluorescence in ImageJ (National Institutes of Health) and pixels counted using the 'Analyse particles' function.

Lipoprotein assay

Lipoprotein abundance was measured using the HDL & LDL/VLDL Cholesterol Assay Kit (Cell Biolabs) as per manufacturer's instructions and based on previously published methods (O'Hare et al. 2014). Briefly, 10 embryos per treatment group were terminally anaesthetised and placed into BHT solution (10 µg/mL, Sigma-Aldrich) and homogenised. Homogenates were centrifuged at 4°C at 2000 x *g* for 5 mins to pellet debris. The supernatant was mixed with an equal volume of precipitation solution to separate the high density lipoprotein (HDL) and low density lipoprotein (LDL) fractions. Each lipoprotein fraction was mixed with an equal volume of reaction mix and quantified by fluorescent plate reader. A standard curve was included in each run to calculate the concentration of lipoproteins within each treatment.

Oil Red O staining

Oil Red O lipid staining on whole mount embryos was completed as previously described (Passeri et al. 2009). Briefly, embryos were individually imaged for bacterial distribution by fluorescent microscopy, fixed, and stained in Oil Red O (0.5% w/v in propylene glycol). Oil Red O staining intensity at sites of infection were quantified in ImageJ and calculated as the pixel density above background tissue.

Molecular analysis of *ldlra* knockdown

RNA was extracted in TRIZOL (Thermofisher) by precipitation and cDNA was synthesised with an Applied Biosystems High Capacity cDNA reverse transcription kit (Thermofisher). PCR was performed with *ldlra*-specific primers (5'-AGAGCTGGAAATGTGACGGA-3' and 3'-CTCATCTGGACGGCATGTTG-5') and visualised by gel electrophoresis.

Quantitative PCR

Quantitative PCR (qPCR) reactions were completed as previously described (Taylor et al. 2008) using Mx3000P real-time PCR systems (Stratagene). Gene-specific primers were generated for *abca1* (5'-AGCTGCTGGTCGAGATCATA-3' and 3'-CTGTCTCACTGCATGCTTGG-5') for comparison against housekeeping gene *actb* (5'-CCTTCCAGCAGATGTGGATT-3' and 3'-CACCTTCACCGTTCCAGTTT-5'). Samples were run in duplicate with reaction specificity confirmed based on the post-amplification dissociation curve.

Statistical analysis

Genstat (VSN International) and Prism (Graphpad) were used to perform statistical testing as indicated. Bacterial burden was examined using Restricted Maximum Likelihood (REML) coupled with Fishers protected LSD; experiment number was included as the random effect to account for variability between experimental replicates. Lipoprotein abundance, Oil Red O staining density and gene expression analysis were analysed using unpaired Student's t-tests.

Results

Infection-induced altered host lipid metabolism is recapitulated in the zebrafish-*M. marinum* infection model

Previous reports have identified that hypercholesterolemia correlates with disease pathology during human *Mtb* infection (Dong et al. 2017). To determine whether these findings were conserved within the zebrafish-*M. marinum* platform, we analysed the total embryo LDL and HDL content at 3 and 5 days post infection (dpi), corresponding to an early infection timepoint and the onset of granuloma necrosis, respectively. Calculation of lipoprotein content revealed a skewing towards LDL (Figure 1A).

Knockdown of *Ldlra* reduces *M. marinum* burden in zebrafish embryos

Infection of macrophages with various species of mycobacteria, including in the zebrafish-*M. marinum* system, increases *LDLR* transcription (Johansen et al. submitted-b; Kim et al. 2010). Given the infection-induced changes in the ligand LDL in our model, we tested the functional relevance of LDLR by morpholino knockdown of the zebrafish *ldlra* gene (O'Hare et al. 2014). Knockdown of Ldlra had no effect on embryo development and editing of the *ldlra* transcript was observed (Figures 1B and S1A). Oil Red O staining for lipids in Ldlra-depleted embryos revealed marked vascular lipid accumulation consistent with previous reports of Ldlra depletion being atherogenic (Figure S1B) (O'Hare et al. 2014).

Following Ldlra-depletion, embryos were infected with fluorescent *M. marinum* and bacterial burden was analysed by fluorometry. Zebrafish embryos depleted of Ldlra displayed a significantly decreased bacterial burden at 3 and 5 days post-infection (dpi) when compared to control embryos (Figures 1C, 1D, S2A and S2B).

Knockdown of Ldlra corrects infection-induced altered host lipid metabolism

Host lipid metabolism is a tightly controlled biological pathway, responsible for addressing the cellular lipid requirements through the regulation of influx and efflux mechanisms. Of the many surface receptors involved in lipid metabolism, LDLR is arguably the most important, playing a key role in driving the uptake of circulating LDL (Cardona et al. 2009).

Following *M. marinum* infection, expression of the LDLR-network and lipid efflux gene *ABCA1* was markedly increased (Figure 2A). Depletion of Ldlra significantly reduced *abca1* transcription, demonstrating a transcriptional conservation of infection-induced lipid metabolism network in our model (Figure 2A).

We hypothesised that infection-induced LDLR is a key node in driving infection-induced hyperlipidaemia, and that depletion of LDLR would prevent infection-induced hypercholesterolemia and the accumulation of lipids within granulomas. Following *M. marinum* infection, Ldlra-deficient embryos displayed a decreased LDL:HDL ratio compared to infected controls at 5 dpi (Figure 2B).

Next, we hypothesised that the combination of reduced potential for LDL uptake and correction of total cholesterol levels would reduce granuloma lipid accumulation in Ldlra-depleted embryos. Granuloma Oil Red O lipid staining density was reduced in infected Ldlra-deficient embryos compared to infected controls demonstrating a functional role for LDLR in directing bacterial-beneficial lipid accumulation during mycobacterial infection (Figures 2C, 2D, S3A and S3B).

Discussion

The hallmark of mycobacterial disease is the formation of granulomas at the site of infection (Ramakrishnan 2012). Foam cells are an important component of granulomas and their transformation is driven by the dysregulation of macrophage lipoprotein influx and efflux (Cardona et al. 2009). These lipid-filled macrophages are deficient in their phagocytic abilities and provide an intracellular carbon-based nutrition source, enabling the intracellular survival of mycobacteria (Cardona et al. 2009). The findings from this study demonstrate host LDLR is co-opted by mycobacterial infection to manipulate host lipid metabolism and foam cell formation, ultimately increasing the susceptibility of the host to mycobacterial infection.

The elevation of host lipids following mycobacterial infection has been well documented in both human and murine *Mtb* infections (Dong et al. 2017; Martens et al. 2008). Recently, we have shown that elevated serum cholesterol is associated with histopathological lesions in sheep and cattle infected with MAP (Johansen et al. submitted-a). The results from the current study are in agreement with previous findings and suggest that hypercholesterolemia may be a conserved trait induced by pathogenic mycobacteria. Furthermore, our results demonstrated that *LDLR* knockdown significantly altered the availability of circulating lipoproteins and decreased Oil Red O staining density, providing strong evidence to suggest that the abundance of neutral lipids and therefore foam cells, was largely decreased as a consequence of *LDLR* depletion.

Host lipid metabolism is a complex pathway involving many transcription factors, surface molecules and feedback mechanisms. In the absence of key components, compensatory pathways are utilised to achieve cellular homeostasis. Expression of *abca1* was increased following *M. marinum* infection, in agreement with previous studies identifying the upregulation of *ABCA1* by mycobacterial infection across multiple host species (Long et al.

2016). Interestingly, there was a notably lower expression in *ldlra*-deficient embryos, presumably due to the decreased efflux of lipids from mycobacteria-infected macrophages as a consequence of the altered lipoprotein abundance.

Collectively, this study provides evidence of conserved infection-induced altered host lipid metabolism in the zebrafish-*M. marinum* model, and highlights a crucial role of *LDLR* in infection susceptibility across host and pathogen species.

Acknowledgements

Drs Anneliese Ashurst and Gayathri Nagalingam for training assistance with laboratory equipment; Dr Kristina Jahn and Sydney Cytometry for assistance with imaging equipment. Special thanks goes to the animal house staff at the Garvan Institute of Medical Research and CSIC.

References

Cardona, P., Allain, S., Altare, F., Kim, M. & Russell, D. G. 2009, 'Foamy macrophages and the progression of the human tuberculosis granuloma', *Nature Immunology*, vol. 10, no. 9, pp. 943-948.

Dong, Z., Shi, J., Dorhoi, A., Zhang, J., Soodeen-Lalloo, A. K., Chen, W., Yin, H., Sha, W., Li, W., Zheng, R., Liu, Z., Yang, H., Qin, L., Wang, J., Huang, X., Wu, C., Kaufmann, S. H. E. & Feng, Y. 2017, 'Hemostasis and lipoprotein indices signify exacerbated lung injury in tuberculosis with diabetes comorbidity', *Chest*, In Press.

Johansen, M. D., De Silva, K., Plain, K. M., Begg, D. J., Whittington, R. J. & Purdie, A. C. submitted-a, 'Sheep and cattle exposed to *Mycobacterium avium* subspecies *paratuberculosis* exhibit altered total serum cholesterol profiles during the early stages of infection', *Veterinary Immunology and Immunopathology.*

Johansen, M. D., de Silva, K., Plain, K. M., Whittington, R. J. & Purdie, A. C. submitted-b, '*Mycobacterium avium* subspecies *paratuberculosis* is able to manipulate host lipid metabolism and accumulate cholesterol within macrophages', *Pathogens and Disease*.

Kim, M. J., Wainwright, H. C., Locketz, M., Bekker, L. G., Walther, G. B., Dittrich, C., Visser, A., Wang, W., Hsu, F. F., Wiehart, U., Tsenova, L., Kaplan, G. & Russell, D. G. 2010, 'Caseation of human tuberculosis granulomas correlates with elevated host lipid metabolism', *EMBO Molecular Medicine,* vol. 2, no. 7, pp. 258-274.

Long, J., Roy, R. B., Zhang, Y. J. J., Antrobus, R., Du, Y. X., Smith, D. L., Weekes, M. P. & Javid, B. 2016, 'Plasma membrane profiling reveals upregulation of abca1 by infected macrophages leading to restriction of mycobacterial growth', *Frontiers in Microbiology,* vol. 7, no., pp. 1086-1097.

Martens, G. W., Arikan, M. C., Jinhee, L., Ren, F., Vallerskog, T. & Kornfeld, H. 2008, 'Hypercholesterolemia impairs immunity to tuberculosis', *Infection and Immunity,* vol. 76, no. 8, pp. 3464-3472.

O'Hare, E. A., Wang, X., Montasser, M. E., Chang, Y. C., Mitchell, B. D. & Zaghloul, N. A. 2014, 'Disruption of ldlr causes increased ldl-c and vascular lipid accumulation in a zebrafish model of hypercholesterolemia', *Journal of lipid research,* vol. 55, no. 11, pp. 2242-2253.

Pandey, A. K. & Sassetti, C. M. 2008, 'Mycobacterial persistence requires the utilization of host cholesterol', *Proceedings of the National Academy of Sciences of the United States of America,* vol. 105, no. 11, pp. 4376-4380.

Passeri, M. J., Cinaroglu, A., Gao, C. & Sadler, K. C. 2009, 'Hepatic steatosis in response to acute alcohol exposure in zebrafish requires sterol regulatory element binding protein activation', *Hepatology,* vol. 49, no. 2, pp. 443-452.

Ramakrishnan, L. 2012, 'Revisiting the role of the granuloma in tuberculosis', *Nature Reviews Immunology,* vol. 12, no. 5, pp. 352-366.

Stinear, T. P., Seemann, T., Harrison, P. F., Jenkin, G. A., Davies, J. K., Johnson, P. D. R., Abdellah, Z., Arrowsmith, C., Chillingworth, T., Churcher, C., Clarke, K., Cronin, A., Davis, P., Goodhead, I., Holroyd, N., Jagels, K., Lord, A., Moule, S., Mungall, K., Norbertczak, H., Quail, M. A., Rabbinowitsch, E., Walker, D., White, B., Whitehead, S., Small, P. L. C., Brosch, R., Ramakrishnan, L., Fischbach, M. A., Parkhill, J. & Cole, S. T. 2008, 'Insights from the complete genome sequence of *Mycobacterium marinum* on the evolution of *Mycobacterium tuberculosis*', *Genome Research,* vol. 18, no. 5, pp. 729-741.

Taylor, D. L., Zhong, L., Begg, D. J., de Silva, K. & Whittington, R. J. 2008, 'Toll-like receptor genes are differentially expressed at the sites of infection during the progression of Johne's disease in outbred sheep', *Veterinary Immunology and Immunopathology,* vol. 124, no. 1-2, pp. 132-151.

Thirunavukkarasu, S., de Silva, K., Plain, K. M. & Whittington, R. J. 2014, 'Role of host- and pathogen-associated lipids in directing the immune response in mycobacterial infections, with emphasis on *Mycobacterium avium* subsp. *paratuberculosis'*, *Critical reviews in microbiology*, vol. no., pp. 1-13.

Traver, D., Herbomel, P., Patton, E. E., Murphey, R. D., Yoder, J. A., Litman, G. W., Catic, A., Amemiya, C. T., Zon, L. I. & Trede, N. S. 2003, 'The zebrafish as a model organism to study development of the immune system', *Advances in Immunology*, vol. 81, no., pp. 253-330.

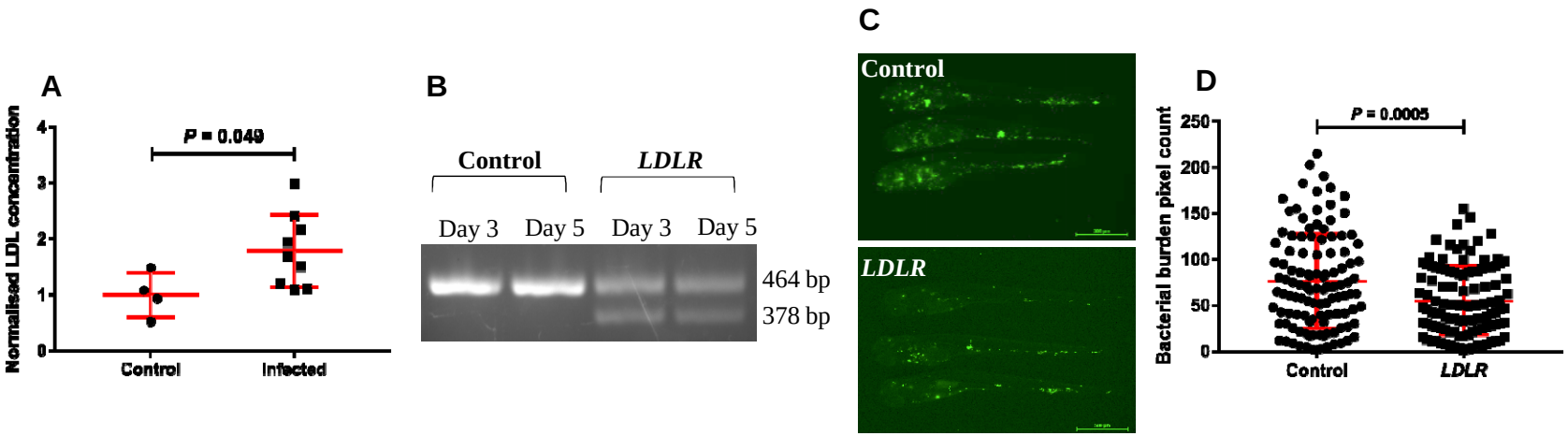

Figure 1: LDL is increased by infection and knockdown of Ldlra reduces *M. marinum* bacterial burden. *A*, Quantification of LDL concentration in wild-type zebrafish embryos at 5 days following *M. marinum* infection. Each data point represents a pooled sample of 10 embryos. *B*, Molecular validation of *ldlra* morpholino efficacy at 3 and 5 days post-treatment. *C*, Representative images of *M. marinum*-wasabi bacterial distribution at 5 days-post infection. Scale bar represents 500 µm. *D*, Quantification of *M. marinum* bacterial burden by fluorometry at 5 days post-infection. Error bars represent standard deviations. Statistical tests for LDL quantification were performed using unpaired Student's t-tests. Analysis of *M. marinum* bacterial burden was completed using REML coupled with Fisher's protected LSD; experiment number was included as random effect. Experiments were completed with 4 independent biological replicates for each panel.

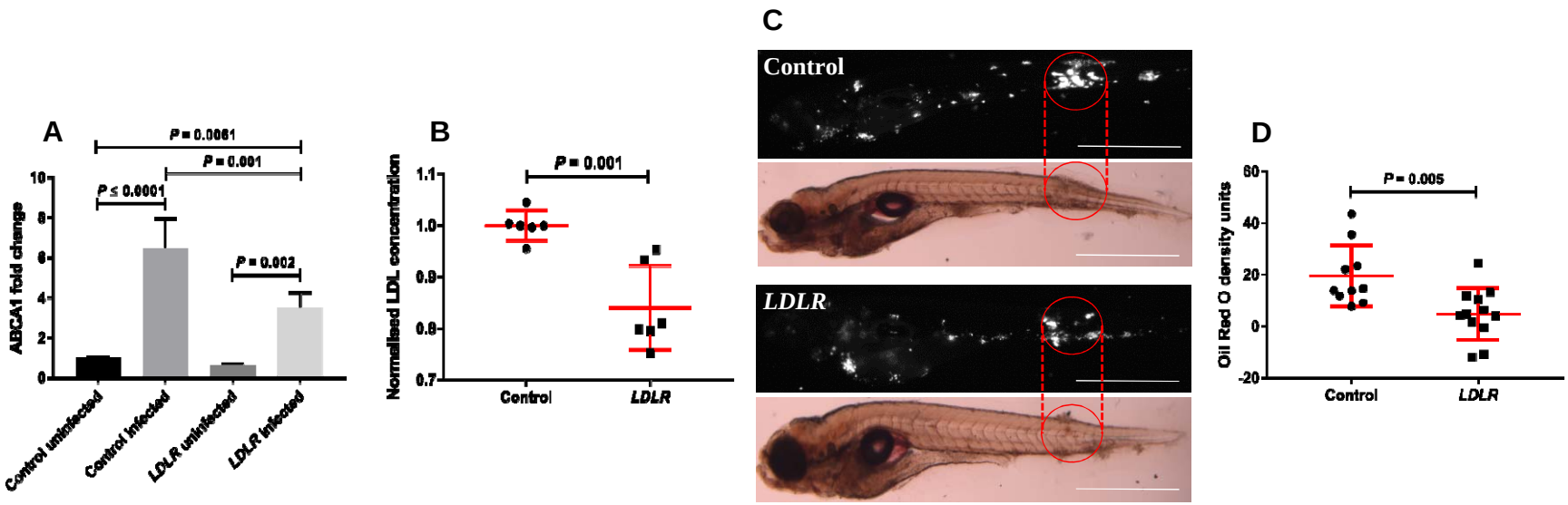

Figure 2: Mycobacterial infection-induced modulation of host lipid metabolism is corrected in Ldlra-deficient embryos. *A*, *abca1* transcript fold change expression at 5 days post-infection measured by qPCR. Each column represents two independent biological replicates completed with technical replicates. *B*, Quantification of LDL concentration in Ldlra-deficient embryos at 5 days-post infection. Each data point represents a pooled sample of 10 embryos completed with four independent replicates. *C*, Representative images of Oil Red O staining density at 5 days post-infection. Red circles indicate areas of embryos with largest foci of infection. Scale bar represents 500 µm. *D*, Quantification of granuloma Oil Red O staining density units at 5 days post-infection. Each data point represents an individual embryo. Error bars represent standard deviation. Gene expression analysis was completed using one-way ANOVA. Analysis of LDL concentration and Oil Red O density units was completed using an unpaired Student's t-test.

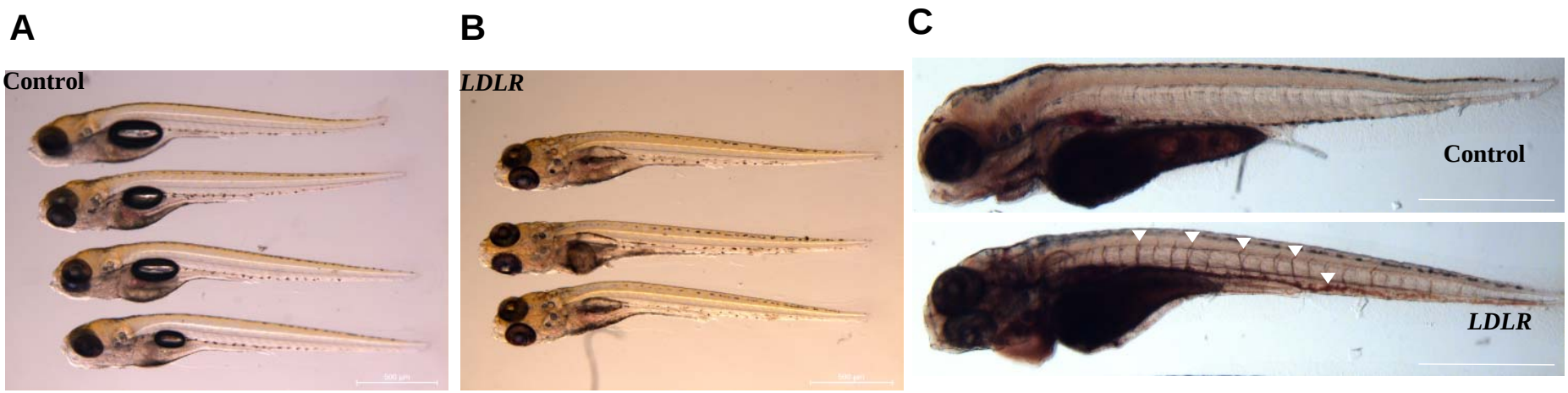

Supplementary figure 1: Knockdown of Ldlra results in extensive lipid accumulation with the vasculature. *A*, Normal morphology and phenotypes at 5 days post-fertilisation. *B*, Embryos deficient in Ldlra show normal phenotypes at 5 days following morpholino treatment. *C*, Embryos deficient in Ldlra display visible lipid abundance within the vasculature following Oil Red O lipid staining. White arrows represent expansive lipid accumulation within the vasculature. Scale bars represent 500 µm.

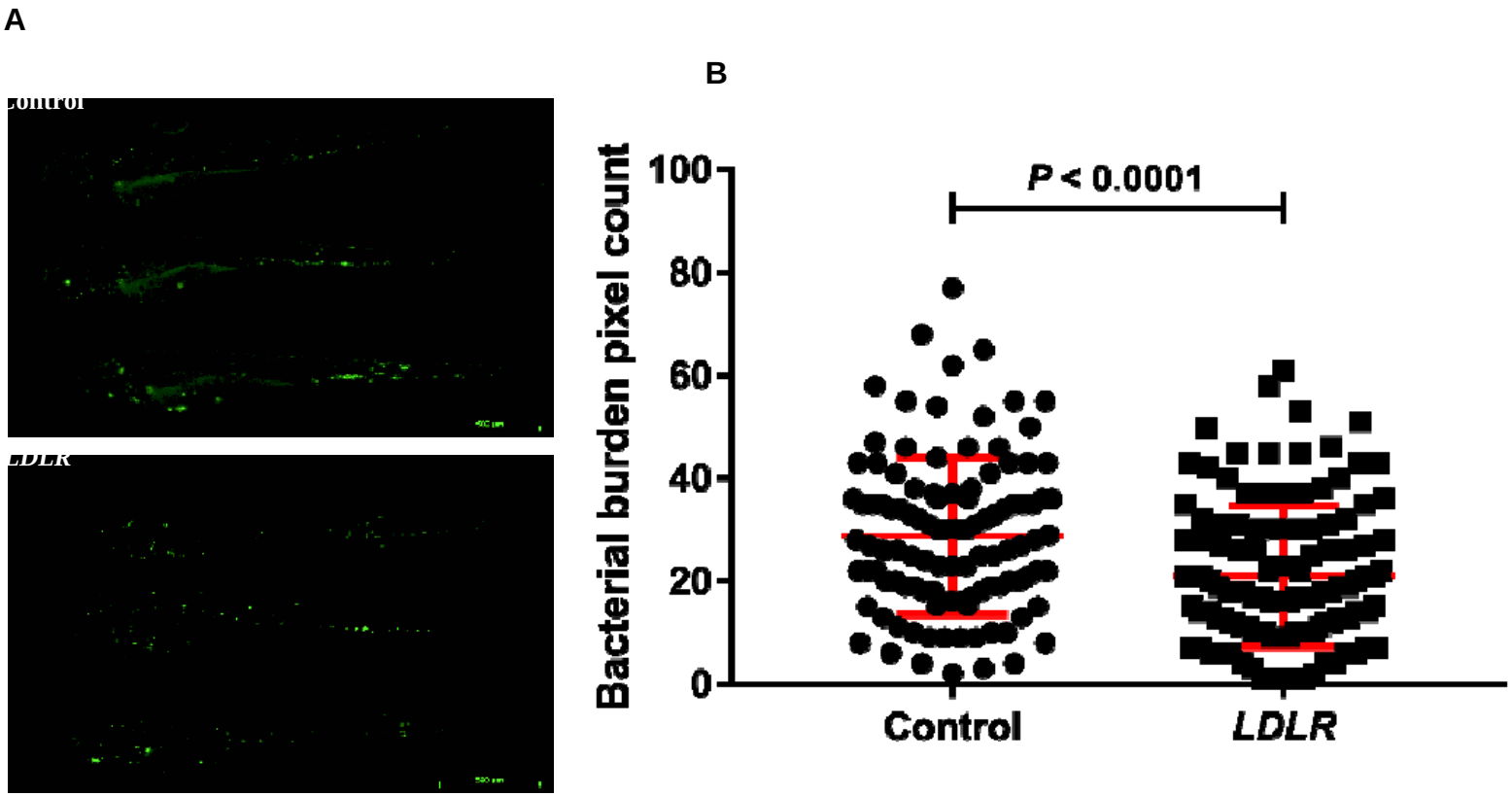

Supplementary figure 2: Bacterial burden is reduced in Ldlra-deficient embryos at 3 days post-infection. *A*, Representative images of *M. marinum* bacterial burden at 3 days-post infection. Scale bars represent 500 µm. Quantification of *M. marinum* bacterial burden at 3 days post-infection. Error bars represent standard deviations. Analysis of *M. marinum* bacterial burden was completed using REML coupled with Fisher's protected LSD; experiment number was included as random effect.

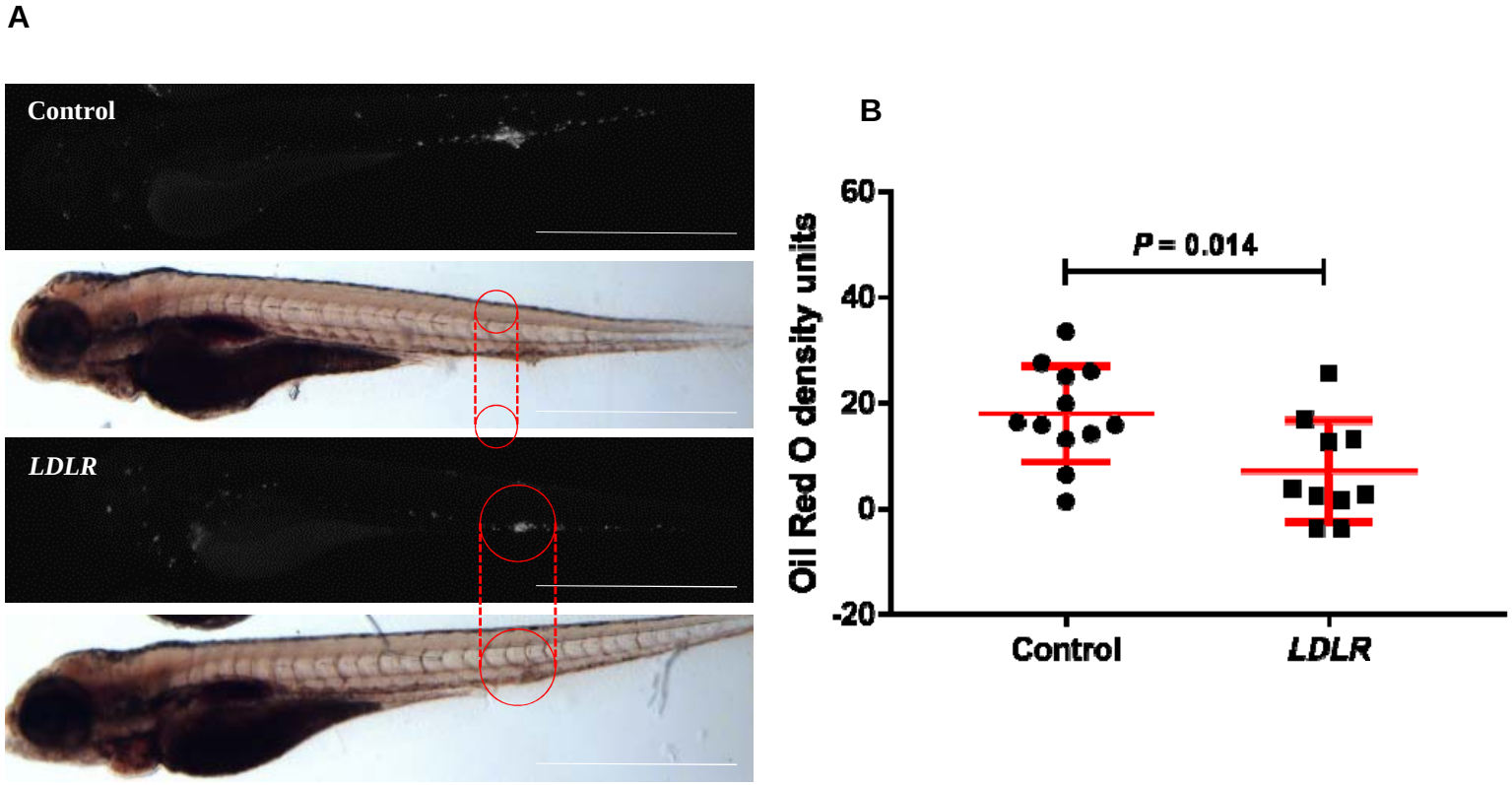

Supplementary figure 3: Granuloma Oil Red O staining is reduced in Ldlra-deficient embryos at 3 days post-infection with *M. marinum*. *A*, Representative images of Oil Red O staining density at 3 days post-infection with *M. marinum.* Scale bars represent 500 µm. *B*, Quantification of Oil Red O density units at 3 days post-infection with *M. marinum*. Each data point represents an individual embryo. Error bars represent standard deviation. Statistical tests were performed using unpaired Student's t-tests.